Bioelectrochemistry 135 (2020) 107579

Contents lists available at ScienceDirect

Bioelectrochemistry

journal homepage: www.elsevier.com/locate/bioelechem

# An electrochemical study of 9-chloroacridine redox behavior and its interaction with double-stranded DNA

Jelena Rupar [a], Mara M. Aleksić [a,*], Vladimir Dobričić [b], Jasmina Brborić [b], Olivera Čudina [b]

[a] University of Belgrade, Faculty of Pharmacy, Department of Physical Chemistry and Instrumental Methods, Vojvode Stepe 450, P.O.Box 146, 11221 Belgrade, Serbia
[b] University of Belgrade, Faculty of Pharmacy, Department of Pharmaceutical Chemistry, Vojvode Stepe 450, P.O.Box 146, 11221 Belgrade, Serbia

ARTICLE INFO

*Article history:*
Received 7 December 2019
Received in revised form 25 May 2020
Accepted 31 May 2020
Available online 3 June 2020

*Keywords:*
9-Chloroacridine redox mechanism
dsDNA-electrochemical biosensor
Interaction
Square wave voltammetry
Molecular docking

ABSTRACT

The electrochemical behavior of 9-chloroacridine (9Cl-A), a precursor molecule for synthesis of acridine derivatives with cytostatic activity, is a complex, pH-dependent, diffusion-controlled irreversible process. Oxidation of 9Cl-A initiates with the formation of a cation radical monomer, continues via the formation of a dimer subsequent oxidation to new cation radical. Reduction of 9Cl-A produces radical monomers which are stabilized by dimer formation. The investigation was performed using cyclic, differential pulse and square wave voltammetry at a glassy carbon electrode. The interaction between 9Cl-A and double-stranded DNA (dsDNA) was investigated using a multilayer dsDNA-electrochemical biosensor and 9Cl-A solutions from $1.0 \times 10^{-7}$M (the lowest 9Cl-A concentration whose interaction with DNA was possible to detect) up to $1 \times 10^{-4}$M. These allowed the binding constant, $K = 3.45 \times 10^{5}\text{M}^{-1}$ and change in Gibbs free energy of the formed adsorbed complex to be calculated. Complex formation was a spontaneous process proceeding via 9Cl-A intercalation into dsDNA inducing structural changes. The intercalation of 9Cl-A into dsDNA was supported by molecular docking analysis.

The combination of simple methodology and the use of biosensors to investigate DNA interactions is a powerful tool to offer insight into aspects of drug design during pharmaceutical development.



## 1. Introduction

Acridines are heterocyclic structures which play an important role in a variety of diseases; that is why they have been widely studied and used clinically as antibacterial, antiparasitic, antiviral, antiseptic and antitumor agents [1,2]. Acridines are good candidates as antitumor agents, since they are able to form complexes with DNA. They are capable of interacting with nuclear DNA in a sequence-specific manner and with biological targets, such as topoisomerase I and II and telomerase [3]. The biological activity of acridines has been attributed to the planarity of the polyaromatic ring structure, which can intercalate within double-stranded DNA leading to stacking and thus interference with cellular functions [1,4]. Amongst the acridines, 9-chloroacridine (9Cl-A Scheme 1, 2) may be especially important due to its possible usage as a precursor molecule for the synthesis of acridine derivatives with a cytostatic activity [5].

Nitrogenous bases and the sugar-phosphate backbone form the targets of the DNA molecule for different biological compounds and drugs, which after interaction (covalent bonds, intercalation, groove binding or electrostatic interactions) cause structural changes in the DNA [6–10]. According to voltammetric and atomic force microscopy (AFM) data [11,12], after the interaction between DNA and the compound, the DNA double helix denatures locally and allows easier interactions between a carbon electrode surface and the DNA bases. AFM measurements [11] have confirmed that the decreases in guanine and adenine oxidation peaks obtained by voltammetric measurements were the result of thicker aggregates formed due to DNA condensation.

In general, binding of drugs to DNA, and DNA damage has been described in the literature through the variation of the electrochemical signal of guanine or adenine [6,13–22]. The electrochemical signal related to a drug–DNA interaction can provide evidence for the interaction mechanism and for the nature and type of the complex formed.

A dsDNA based electrochemical biosensor [23,24] has been used as a tool for studies of dsDNA interaction with many different small molecules, including drugs and hazardous compounds. Differential pulse voltammetry [25–27] was reported as a useful method for this type of investigation due to its capability of detecting changes in the DNA double-helical structure with greater sensitivity [28] compared with other methods. This type of biosensor is formed by the immobilization of the dsDNA on an electrode surface and

* Corresponding author.
*E-mail address:* mara.aleksic@pharmacy.bg.ac.rs (M.M. Aleksić).

https://doi.org/10.1016/j.bioelechem.2020.107579
1567-5394/

the method used for its formation determines the accessibility of the DNA to the analysed compound. For mono or multilayer sensors several immobilization procedures may be used, including evaporation or electrostatic adsorption. The multilayer dsDNA-electrochemical biosensor represents an electrode covered with dsDNA by successive deposition of predetermined dsDNA solution on its surface [29].

Research into DNA binding interactions with drug molecules contributes to understanding the mechanisms behind drug action as well as the design of novel DNA-targeting drugs. Apart from our previous studies [30,31] no other data exist concerning electrochemical studies of 9-chloroacridine (9Cl-A) nor its interaction with DNA. Electroactivity of other acridine derivatives was previously confirmed by different voltammetric methods using diverse electrodes [23,32–34]. Polarography and voltammetry were used decades ago for the prediction of acridine (and some of its derivatives), oxidation and reduction mechanisms [35–39].

We have used cyclic (CV), differential pulse (DPV) and square wave (SWV) voltammetry to examine the oxidation and reduction mechanisms of 9Cl-A at different pH values in acidic and basic conditions. In addition, the interaction between 9Cl-A and calf thymus double stranded DNA (dsDNA) was studied using a multilayer dsDNA modified glassy carbon electrode (GCE) by observing the decrease in adenine oxidation current obtained from SWVs.

The aim of this current study was to provide new data concerning 9Cl-A oxidation and reduction mechanisms, to clarify the nature and the mode of interaction between 9Cl-A and dsDNA, to evaluate the binding constant of the formed adsorbed complex and the value of the Gibbs free energy change using simple electroanalytical methodology and biosensors. Experimental data were supported by molecular docking analysis.

## 2. Experimental

### 2.1. Apparatus

Voltammetric measurements were performed using an μAutolab analyzer (Eco Chemie, Utrecht, The Netherlands) operating with GPES 4.9 software. A three electrode cell was used with a glassy carbon electrode (GCE, $d$ = 3 mm, CH Instruments, Inc., Austin, TX, USA) as a working electrode, Ag/AgCl as a reference (3.00 M KCl) and Pt as an auxiliary electrode. An aqueous slurry of $Al_2O_3$ powder (particle size 0.05 μm) was used for GCE polishing on a smooth polishing pad. After polishing, the GCE was sonicated in double distilled water for 2 min and then in absolute ethanol for 2 min. An ultrasonic bath 'Iskra' UZ 4R (Sentjernej, Slovenia) was used for sonication. pH measurements were performed using a PHM 220 pH meter with a combined electrode Radiometer GK2401B. A SCALTEC SBC 31 balance was used for weight measurements.

### 2.2. Reagents

9-chloroacridine (9Cl-A) and calf thymus double stranded DNA (dsDNA, $MW_r$ = 10 – 15 × $10^6$) were obtained from Sigma-Aldrich and were used without further purification. A stock solution of 1.0 × $10^{-3}$ M 9Cl-A was prepared in absolute ethanol and stored at 4 °C. Final concentrations of 2.5 × $10^{-4}$ M 9Cl-A for CV, DPV and SWV measurements and different concentrations ranging from 1.0 × $10^{-7}$ M to 1.0 × $10^{-4}$ M for the examination of 9Cl-A-DNA interaction were obtained by diluting the stock solution with appropriate supporting electrolytes. All the chemicals were of analytical grade quality. The stock solution of dsDNA, 73.95 μg $mL^{-1}$, was prepared by dissolving in acetate buffer, pH 4.6.

A HCl/KCl system of 0.10 M ionic strength for pH value of about 2.0 [40], acetate buffers for pH values of 3.5, 4.6, 5.2 (sodium acetate in the solution of acetic acid), phosphate buffers for pH values of 6.2, 7.0, 8.1 (disodium hydrogen phosphate dihydrate dissolved with sodium dihydrogen phosphate monohydrate) and ammonia buffer for pH value of 9.0 ($NH_3$ dissolved with ammonium chloride) were prepared according to the literature using analytical grade reagents and double distilled water [40,41]. The ionic strength of all solutions was 0.10 M. Experiments were performed at room temperature (25 °C). Nitrogen-saturated solutions were obtained by passing high purity nitrogen gas for at least 10 min through the solution prior to experiments and maintained using a flow of gas over the solution during the voltammetric experiments to eliminate oxygen from the solutions.

### 2.3. ds-DNA – Electrochemical biosensor preparation

The multilayer dsDNA biosensor [42,43] was prepared by covering the surface of glassy carbon electrode successively with three drops of dsDNA (5 μL, concentration 73.95 μg $mL^{-1}$). The electrode surface was dried under an atmosphere of nitrogen after placing each drop. When the third drop was dried, the biosensor was washed with deionized water (to eliminate the excess of unbounded, free dsDNA molecules) and immersed in 9Cl-A solution for variable incubation times. After removal from the solution, the biosensor was washed with deionized water and placed in the electrochemical cell. The dsDNA–9Cl-A interaction was examined at different concentrations of 9Cl-A (1.0 × $10^{-7}$ M – 1.0 × $10^{-4}$ M) and for different periods of incubation time (5–30 min) using SWV.

During the DNA biosensor preparation different parameters such as drying time, drop volume, DNA concentration and pH were optimized. Reproducibility testing of the prepared biosensors was based on current and potential measurements obtained with five biosensors. The standard deviation for peak potential of 3 mV and standard deviation for peak current of 6 – 7 nA showed satisfactory results. Reproducibility of the sensor preparation method was expressed by the relative standard deviation (RSD) being 0.21% and 0.22% for peak dG and dA potential, and 7.5% and 4.6% for peak dG and dA current, respectively. Results are presented in Table S1 in Supplementary Material. In this way, biosensor stability was confirmed by monitoring the biosensor signal in acetate buffer pH 4.6 for 30 min.

### 2.4. Electrochemical measurements

Cyclic voltammetry (CV) was performed starting from 0 V, increasing to + 1.6 V and decreasing to −1.3 V (*vs.* Ag/AgCl, 3 M KCl), as well as in reverse. Scan rate was adjustable, ranging from 0.01 V $s^{-1}$ up to 0.1 V $s^{-1}$ with step potential of 0.005 V. Differential pulse voltammetry (DPV) was used with the following conditions: Step potential 0.005 V, modulation amplitude 0.05 V, modulation time 0.05 s and interval time 1 s. Conditions for square wave voltammetry (SWV) were: Frequency 25 Hz, step potential 0.001 V, effective scan rate of 0.025 V $s^{-1}$ and pulse amplitude of 0.005 V.

The DP and SW voltammograms presented are baseline-corrected using moving average application with a step window of 0.005 V. When necessary, the experimental voltammograms were smoothed using a Savitsky-Golaz smoothing algorithm. Corrected voltammograms were only used for better visualization and graphical presentation of peaks. However, this mathematical treatment reduces peak intensity in some cases. All the values for peak current used and presented in all plots were determined from the original, untreated voltammograms.

### 2.5. Molecular docking analysis

Previous studies showed that a potent antineoplastic agent amsacrine (an aminoacridine derivative structurally comparable to 9Cl-A) intercalates into dsDNA [44]. 3D coordinates of the DNA/amsacrine/topoisomerase II complex were obtained from the Brookhaven protein data bank (PDB code: 4g0u) [45] and used in this study. For the purpose of research presented in this work topoisomerase II was not of interest, and hence it was not taken into consideration in docking analysis. The file obtained from Brookhaven protein data bank was prepared using Discovery Studio 4.5.0 [46] and molecular docking analysis was performed in AutoDock Vina [47]. The mass center of the receptor of interest catalytic site with grid spacing of 0.0375 nm was used for building a grid of 10, 10, and 10 points in x-, y-, and z- directions, respectively. The exhaustiveness parameter was set to 8. Re-docking of the co-crystallized ligand into the 3D structure of the receptor was attempted with the aim to validate docking analysis. Docking analysis was proved valid, considering the obtained RMSD value (<0.2 nm).

## 3. Results and discussion

Electrochemical investigation of $2.5 \times 10^{-4}$ M 9Cl-A in nitrogen-saturated acetate buffer pH 3.5, was performed using CV at GCE. Voltammograms were recorded over three successive scans during which the potential changed from 0.0 V (*vs.* Ag/AgCl, 3 M KCl) towards + 1.6 V (Fig. 1A) and − 1.3 V (Fig. 1B). When the potential was changed toward positive values, one anodic peak (Ia) appeared at $E_{p,Ia}$ = 1.06 V and after changing the potential direction, a cathodic peak (Ic) appeared at $E_{p,Ic}$ = − 0.68 V. In the second and third scans, beside the two peaks mentioned, an additional small, poorly developed, oxidation peak appeared at a potential around + 0.5 V (*vs.* Ag/AgCl, 3 M KCl). Oxidation and reduction peaks Ia and Ic were always present (in all three scans) no matter which direction was chosen to record the voltammogram.

The influence of initial and vertex potential in the ranges between −1.3 V and 0 V, 0.0 V to +1.6 V, as well as +0.5 V to +1.6 V was tested. There were no differences in the voltammetric curves registered (data not shown), comparing to the overall scans presented in Fig. 1.

Background electrolyte did not affect the 9Cl-A voltammetric peaks in any way. This is shown in Fig. 1 (voltammogram of acetate buffer pH 3.5, *I* 0.10 M, recorded under the same conditions as 9Cl-A).

According to the above results, 9Cl-A undergoes separate processes of oxidation yielding peak Ia and reduction yielding peak Ic. The reduction product seems to be capable of being oxidized, yielding a small peak at +0.5 V (*vs.* Ag/AgCl, 3 M KCl).

Since oxidation and reduction of 9Cl-A occur independently, these processes were investigated separately.

### 3.1. Oxidation

During scanning of the potential towards the positive potential limit the anodic peak (Ia) occurred. After changing the direction of the scan, no corresponding reduction peak in the reverse scan was observed, meaning that the oxidation process of 9Cl-A was irreversible. The pH dependence of 9Cl-A oxidation was investigated in a pH range from 2.0 to 9.0 using CV, Fig. 2. The intensity of the Ia peak current decreased in neutral medium. At pH > 9.0 it was no longer observed (data not shown).

The shift in the oxidation peak to less positive potentials with increasing pH indicated a facilitated oxidation process in less acidic conditions which is in accordance with increasing nucleophilicity of solution at higher pH. The peak potential dependence was linear throughout the investigated pH range according to the equation: $E_{p,\ Ia}$ (V) = − 0.063 pH + 1.27 ($R^2$ = 0.994). A slope of 63 mV per pH unit suggested that the oxidation process of 9Cl-A required the same number of electrons and protons [48].

The calculated value for the difference between peak potential and half-height peak potential was about 40 mV. Considering the equation:

$$\left|E_p - E_{p1/2}\right| = 47.7/(\alpha n_\alpha) \quad (1)$$

where $\alpha$ is the charge transfer coefficient and $n_\alpha$, the number of electrons transferred in the rate determining step [49,50], the calculated value was $\alpha n_\alpha \approx 1.2$. Bearing in mind that for an irreversible process the transfer coefficient value should be less than or equal to 1 (actually between 0.3 and 0.7), it follows that $n_\alpha$ which is an integer, must be>1 and therefore the rate determining step should involve 2 electrons.

The change in peak Ia current, which firstly increased with pH and then decreased at pH > 5, indicated that the electrooxidation process was accompanied by two reactions. First, electron transfer was probably followed by an intermediate chemical step; and second, successive electron transfer occurred.

The scan rate effect on the 9Cl-A oxidation peak potential and current was monitored both at pH 4.5 and 7.0. The positive peak potential shift of the anodic peak with an increase in scan rate indicated that this oxidation process was irreversible [51,52]. This is in accordance with the shape of the voltammograms. The peak current of 9Cl-A increased linearly with the square root of $v$ at both pH 4.5 ($I_{p,Ia}$ (μA) = 8.72 $v^{1/2}$ (V $s^{-1}$)$^{1/2}$ + 0.045; $R^2$ = 0.994), and

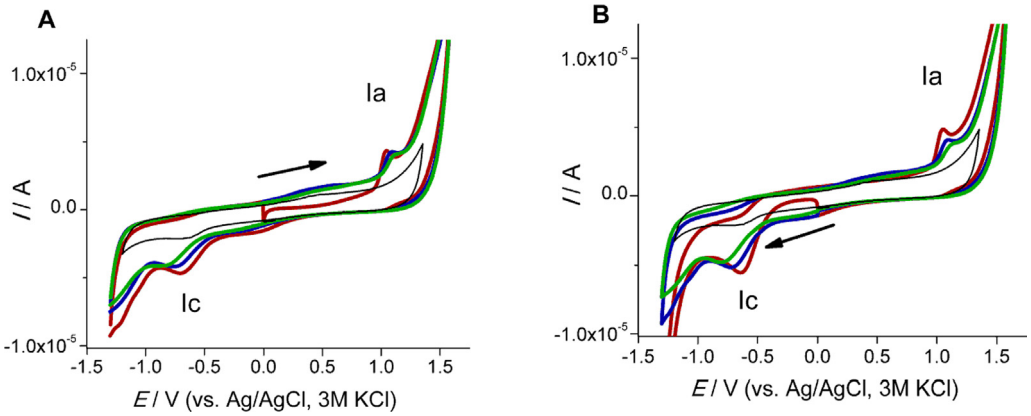


**Fig. 1.** The CVs of $2.5 \times 10^{-4}$ M 9Cl-A in acetate buffer, pH 3.5, recorded in potential range between −1.3 V and + 1.6 V, starting from 0.0 V: (A) in the positive direction and (B) in the negative direction; first (——), second (——) and (——) third scan and (——) acetate buffer, pH 3.5; at $v$ = 50 mV $s^{-1}$.

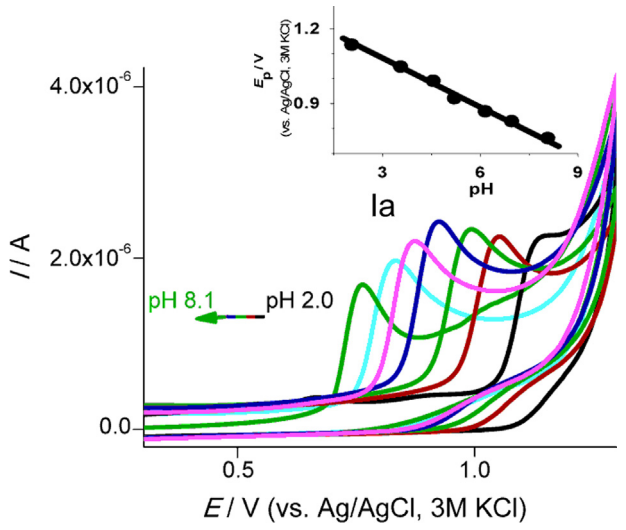


**Fig. 2.** The CVs of 2.5 × $10^{-4}$ M 9Cl-A, first scan plotted as a function of pH of the supporting electrolyte; Inset is a plot of $E_p$ *vs.* pH for oxidation peak Ia (y = –0.063 × + 1.27; $R^2$ = 0.994); $v$ = 20 mV $s^{-1}$.

pH 7.0 ($I_{p,Ia}$ (μA) = 7.67 $v^{1/2}$ (V $s^{-1}$)$^{1/2}$ + 0.222; $R^2$ = 0.996) (Fig. S1 in Supplementary Material) indicating that the oxidation process was diffusion controlled [53–55]. This is confirmed by the log $I_{p,Ia}$ *vs.* log $v$ linear dependence, with slope values of 0.49 and 0.44 (for pH 4.5 and 7.0, respectively), which are close to the theoretical value of 0.5 for a diffusion-limited process.

In addition to diffusion of electroactive material, some adsorption of the electroactive material also took place. The above-mentioned equations, $I_{p,Ia}$ = f ($v^{1/2}$) indicated a small intercept. According to Fig. 1. the oxidation peaks decreased from the first to the second and to the third cycles. This phenomenon may have been attributed to consumption of the adsorbed 9Cl-A oxidation product on the electrode surface.

The peak current for a diffusion-controlled irreversible process is given by the equation:

$$I_p(A) = 2.99 \times 10^5 n(\alpha n_\alpha)^{1/2} ACD^{1/2} v^{1/2} \quad (2)$$

where $n$ represents the number of electrons transferred during the oxidation, $A$ is the electrode surface area in $cm^2$, $D$ is diffusion coefficient in $cm^2$ $s^{-1}$, $C$ is concentration in mol $cm^{-3}$ and $v$ is scan rate in V $s^{-1}$ [49]. The GCE electroactive area was determined previously for the electrochemical reaction of the ferro/ferricyanide redox system according to the Randles-Sevcik equation for a reversible, diffusion-controlled process at a temperature of 25.0 °C. The value of the working electrode electrochemically active surface area was calculated to be $A$ = 0.052 $cm^2$ [56]. From the slope of $I_p$ = f ($v^{1/2}$), which was found to be 8.72 μA/(V $s^{-1}$)$^{1/2}$, the diffusion coefficient of 9Cl-A at pH 4.5 was determined to be $D_{9Cl\text{-}A}$ = 1.06 × $10^{-6}$ $cm^2$ $s^{-1}$. In neutral medium, at pH 7.0 the slope of $I_p$ = f ($v^{1/2}$) was 7.67 μA/(V $s^{-1}$)$^{1/2}$ and accordingly diffusion coefficient $D_{9Cl\text{-}A}$ = 8.1 8 × $10^{-7}$ $cm^2$ $s^{-1}$.

The effect of scan rate on 9Cl-A oxidation peak potential was examined with the aim to investigate the existence of a chemically coupled reaction. The $E_{p,Ia}$ *vs.* log $v$ plot (Fig. S2, Supplementary Material) obtained for the oxidation process resulted in a linear relationship ($E_{p,Ia}$ (V) = 0.021 log$v$ (V $s^{-1}$) + 0.86; $R^2$ = 0.978) with slope of 21 mV, characteristic for an intermediate chemical reaction such as a dimerization process [57].

To investigate the effect of pH, DPV was performed in 2.5 × $10^{-4}$ M solutions of 9Cl-A in a range of pH from 2.0 to 9.0 (Fig. 3A). A stable well shaped oxidation peak Ia was obtained, as seen in CV. However, unlike CV, in DP voltammograms, an additional peak

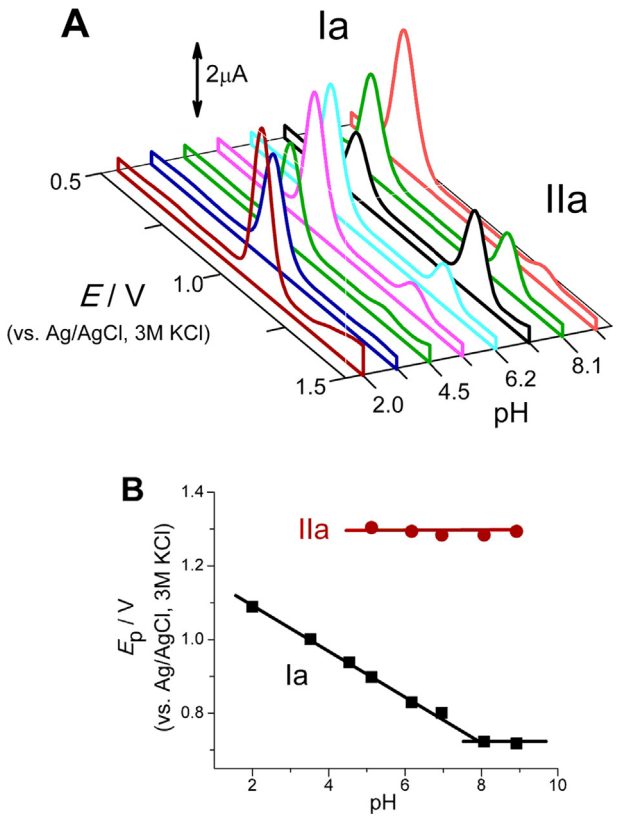


**Fig. 3.** (A) 3D plot of DP voltammograms of 2.5 × $10^{-4}$ M 9Cl-A recorded at different pH; (B) Plot of $E_p$ *vs.* pH (y = –0.060 × + 1.21; $R^2$ = 0.998); ■ – peak Ia, ● – peak IIa.

(IIa) appeared at pH > 5.0, at high positive potentials ($E_{p,IIa}$ ≈ 1.3 V (*vs.* Ag/AgCl, 3 M KCl)). Strong pH dependency was demonstrated only for peak Ia, while the position of peak IIa was pH independent (Fig. 3B).

The variation of the 9Cl-A oxidation peak current with pH was a measure of the variation of the electron transfer rate constant with varying electrolyte solution pH, and always occurs when there is an electron and a proton transfer. The main oxidation peak Ia was shifted to a less positive potential with increasing pH. The slope of the $E_p$ *vs.* pH curve of 60 mV/pH ($E_{p,Ia}$ (V) = – 0.060 pH + 1.21; $R^2$ = 0.998), showed that this oxidation process involved an equal number of electrons and protons. The pH independency of peak IIa potential indicated that protons were not involved in this process.

The half peak width ($W_{1/2}$) values obtained from DPVs were used for the determination of the number of electrons, $n$, involved in the oxidation process using the following equation [49]:

$$W_{1/2} = \frac{3,52RT}{\alpha nF} \quad (3)$$

With increasing pH, width at half-height, the $W_{1/2}$ of peak Ia changed and was in the range from 0.083 V to 0.098 V. According to the literature [52], the transfer of one electron corresponds to a theoretical value of $W_{1/2}$ = 90 mV, so our results showed that in the oxidation process one electron and one proton were transferred.

The oxidation peak IIa that appeared only at 5.0 < pH < 9.0 exhibited the highest peak current in neutral medium. Taking into consideration that peak potential is independent of pH, it is expected that protons do not participate in this oxidation process. The measured value for $W_{1/2}$ was always 0.088 V (independent of pH) and almost equaled the theoretical value of the transfer of

one electron. Therefore, the oxidation step corresponding to peak IIa, occurs with the transfer of one electron only.

When the results obtained by CV and DPV were compared, it could be assumed that the overall oxidation process of 9Cl-A involved transfer of two electrons which could be explained as two one-electron steps (DPV method).

SWV is more sensitive than other voltammetric techniques and it is often used for reversibility predictions [58,59] since oxidation and/or reduction peaks can be registered in the same experiment. SW voltammograms of $2.5 \times 10^{-4}$ M solutions of 9Cl-A at pH 4.5 and 6.2 (presented at Fig. S3 in Supplementary Material) showed results similar to that seen by DPV. One oxidation peak in acidic medium ($E_{p,Ia}$ = 0.97 V) (*vs.* Ag/AgCl, 3 M KCl) and two anodic peaks at pH 6.2 ($E_{p,Ia}$ = 0.86 V, $E_{p,IIa}$ = 1.33 V) (*vs.* Ag/AgCl, 3 M KCl) could be seen in the net current ($I_{tot}$, black line). The same direction of the forward and reverse current components ($I_f$ - red line; $I_b$ – green line) demonstrated the irreversible nature of the 9Cl-A oxidation processes [60,61] which was in line with CV.

### 3.2. Reduction

Reduction was investigated by CV in $2.5 \times 10^{-4}$ M 9Cl-A, in different buffer solutions with pH ranging from 2.0 to 8.0. Peak Ic was present only in acidic solutions, and its potential was shifted to more negative potentials, following the equation $E_{p,Ic}$ (V) = − 0.062 pH − 0.40 (Fig. 4).

The calculated slope, approximately − 60 mV per pH unit, corresponded to the 9Cl-A reduction process involving the same number of electrons and protons [48]. No oxidation peak was observed upon scanning in the positive direction. This indicated that reduction of 9Cl-A was an irreversible process (Fig. 4).

Considering that the difference between peaks potential and potential at their half height $|E_{p,Ic} - E_{p1/2,Ic}|$ was in the range from 93 mV to 107 mV (depending on pH and scan rate), the reduction of 9Cl-A most likely occurred via transfer of one electron and one proton.

CVs were also obtained at different scan rates at pH 4.5. Cathodic shift in reduction peaks with increasing scan rate indicated that the reduction process was controlled by mass transport. This statement was verified by the linear dependency of peak current on the square root of scan rate [53–55] which was calculated to be $I_{p,Ic}$ (μA) = − 2.35 $v^{1/2}$ (V $s^{-1}$)$^{1/2}$ – 0.212; ($R^2$ = 0.964). The diffusion controlled nature of the reduction process was confirmed by the log $I_{p,Ic}$ *vs.* log *v* linear dependence, with a slope value of 0.36.

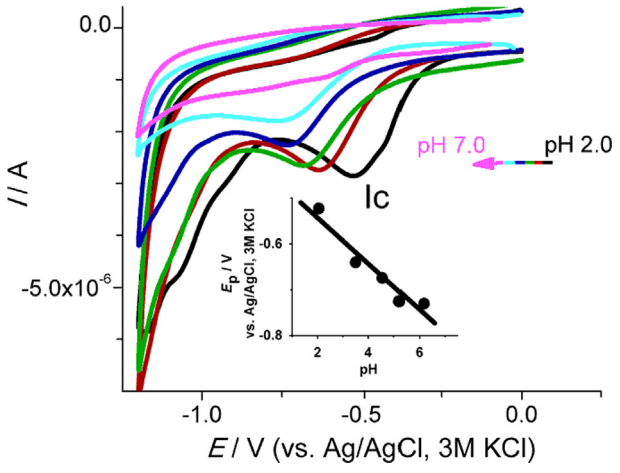


**Fig. 4.** The CVs of $2.5 \times 10^{-4}$ M 9Cl-A, first scan plotted as a function of pH of the supporting electrolyte; Inset is a plot of $E_p$ *vs.* pH for reduction peak Ic (y = – 0.062 × – 0.40; $R^2$ = 0.982); *v* = 50 mV $s^{-1}$.

The effect of scan rate on 9Cl-A Ic reduction peak potential was examined. The plot $E_{p,Ic}$ *vs.* log *v* (Fig. S2, Supplementary Material) yielded a relationship $E_{p,Ic}$ (V) = 0.028 log*v* (V $s^{-1}$) − 0.69; ($R^2$ = 0.953) with a slope of 28 mV, which was a little higher than expected for a dimerization process [57], but still an indicative parameter for such a chemical step following electron transfer.

Using the same methodology already presented for the oxidation process, i.e. applying the Randles-Sevcik equation for an irreversible, diffusion controlled reduction process, the diffusion coefficient of 9Cl-A at pH 4.5 was determined to be $D_{9Cl\text{-}A}$ = 7.63 × $10^{-7}$ $cm^2$ $s^{-1}$.

The pH influence on the 9Cl-A ($c = 2.5 \times 10^{-4}$ M) reduction process was studied using DPV between pH 2.0 and 8.0. In all the electrolytes used, the DP voltammograms indicated reduction peak $I_c$, as presented in Fig. 5A. With increasing pH, peak current intensity decreased and peak potential shifted towards more negative values. The peak potential dependance on pH was linear and followed the relationship:

$E_{p,Ic}$ (V) = − 0.064 pH − 0.28 (Fig. 5B).

A slope of − 0.064 V per pH unit concurred with CV results for the reduction process that happened with the transfer of the same number of electrons and protons. According to the measured width at half-height of the peak that was $W_{1/2}$ > 100 mV, reduction occurs with the transfer of one electron and one proton.

At pH > 5 the principal DPV reduction peak lost its sharpness. With further pH increase it deconvoluted. The presence of the second reduction peak, suggested another consecutive electron transfer.

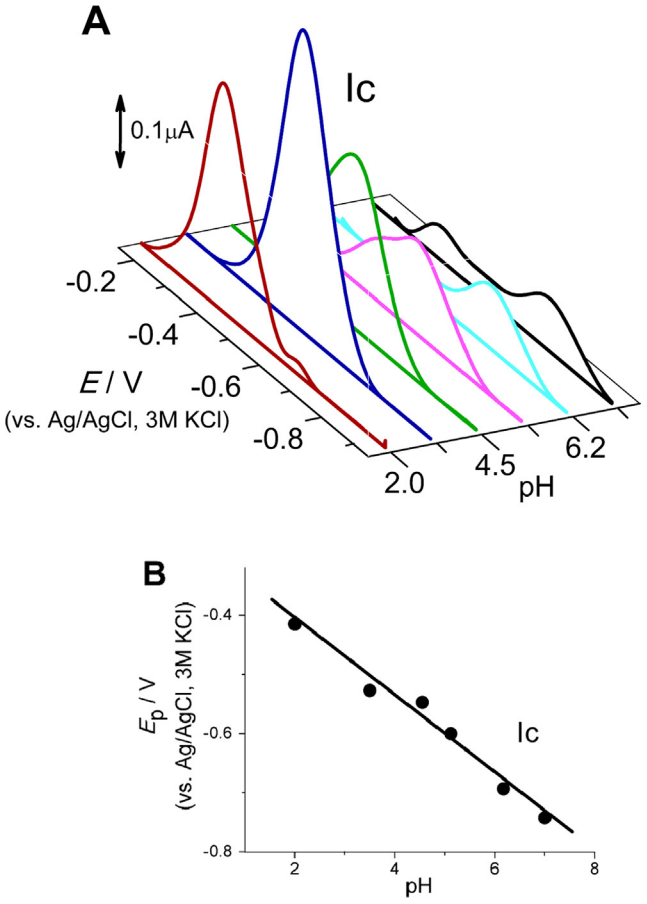


**Fig. 5.** (A) 3D plot of DP voltammograms of $2.5 \times 10^{-4}$ M 9Cl-A reduction recorded at different pH; (B) Plot of $E_p$ *vs.* pH (y = –0.064 × − 0.28; $R^2$ = 0.972); ● – peak Ic.

SW voltammograms from a 2.5 × $10^{-4}$ M solution of 9Cl-A at pH 4.5 (Fig. S4 Supplementary Material) recorded net current ($I_{tot}$) reduction peak ($E_{p,Ic}$ = -0.54 V (*vs.* Ag/AgCl, 3 M KCl)) together with the forward ($I_f$) and backward ($I_b$) current components. It was clear that forward and backward components of the total current were in the same direction [62,63], indicating the irreversible nature of the reduction process of 9Cl-A.

### 3.3. Oxidation and reduction mechanism

Based on the electrochemical data presented, and supported by the fact that 9Cl-A has a planar structure, mechanisms of 9Cl-A oxidation and reduction are proposed.

The oxidation process, according to the CV results, requires two electrons and two protons, whereas using DPV oxidation takes place as two one electron processes. The change in CV oxidation peak current with pH suggested that two consecutive electron transfer reactions were separated with an intermediate chemical step (dimer formation).

A monomer radical cation is produced in the first step after irreversible electron transfer at a potential of ≈ +1.0 V (*vs.* Ag/AgCl, 3 M KCl) with loss of one electron, Scheme 1-A. After the unpaired electron is delocalized in the radical cation, the attack site of the 9Cl-A cation radical may be positions 1 or 3 while positions 4a and 9 are less likely due to steric hindrance (Scheme 1-C). Therefore, it may be assumed that two 9Cl-A cation radical monomers would dimerize (upon formation of a C-N bond) which then continues with the second consecutive electron transfer, as presented in Scheme 1-A, forming a new cation radical.

It may be assumed that the non-protonated form of the dimer, which is dominant at higher pH values, more easily looses electrons compared to its protonated form, which causes formation of a new cation radical (Scheme 1-B). Therefore, the DPV results obtained between pH 5.0 and 9.0 indicating another peak appear-

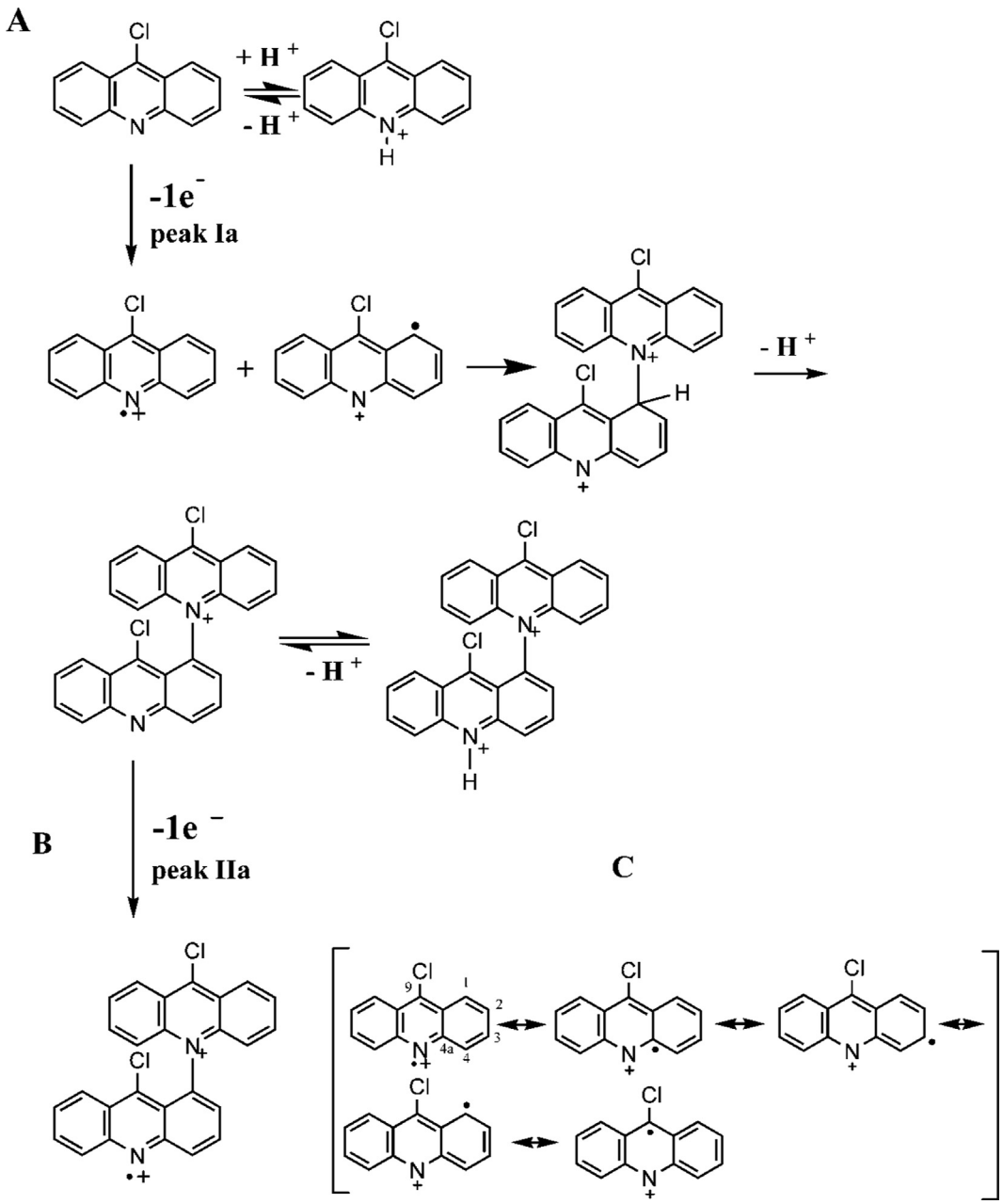


**Scheme 1.** (A, B) Proposed mechanism for oxidation of 9Cl-A; (C) Resonance structures of 9Cl-A radical cation.

ing at a potential of ≈ 1.3 V (*vs.* Ag/AgCl, 3 M KCl) represented the second electron transfer step.

Electrochemically initiated dimerization, as a chemical step taking place between electron transfer steps, was experimentally confirmed by the slope of $E_{p,Ia}$ *vs.* log *v* plot and a value of 21 mV.

Formation of the monomer radical upon oxidation has already been reported for acridine orange [64] and other acridine derivatives [35]. The proposed mechanism concurs with suggested oxidation of similar substances, including acridine which continues via the formation of radical cation monomers, dimers and even tetramers [36] and hexamethylacridine, where an oxidation product has been isolated, and via mass spectrometry it was identified as an acridine type dimer [35].

Reduction of 9Cl-A occurs irreversibly, involving one electron and one proton, resulting in radical formation. The proposed reduction mechanism is presented in Scheme 2. The formed radical is not stable and dimerization is postulated. Due to resonance, different positions may contribute to the dimerization. Steric hindrance makes position 4a less likely for dimerization compared to positions 1 and 3. Therefore it can be assumed that two 9Cl-A radical monomers form a dimer, supported by the resulting slope of $E_{p,Ic}$ *vs.* log *v* plot.

The reduction of acridines was previously studied using different electrodes in different solutions [37–39]. The investigators concluded that it led to the formation of intermediate a semiquinone radical which concurs with our results.

### 3.4. 9-Chloroacridine - dsDNA interaction

Based on the fact that some acridine derivatives can interact with DNA and that 9Cl-A molecule has a planar structure, it is expected that 9Cl-A will show affinity towards DNA. The operational principle of an electrochemical DNA biosensor is based on changes in oxidation signals of both DNA bases and interacting molecules upon the formation of DNA-molecule complexes. For that reason it was important to investigate the mechanism and nature of the 9Cl-A oxidation process in detail, in order to use this principle for detection, monitoring and explanation of the interaction process.

Besides being very advantageous in electroanalysis, SWV was employed in our current study because it offers better resolved voltammograms, less distorted by capacitive effects and more sensitive to electrode kinetics than cyclic voltammograms. Analysis is performed at higher speed, electroactive species are less consumed compared to DPV [65] and problems with electrode surface poisoning are reduced [66].

dsDNA oxidation studies using the DPV method are numerous [4,13,23,26,67]. Despite the above-mentioned published references, we chose to work with SWV. dsDNA oxidation was studied at pH 4.6 (acetate buffer, *I* 0.10 M) and pH 7.0 (phosphate buffer, *I* 0.10 M). The obtained SW voltammograms are shown in Fig. 6 (pH 4.6 - red line, pH 7.0 - black line). Although pH 7.0 was close to physiological pH (and for that matter significant), performing the experiments at pH 4.6 was more convenient for two reasons. Firstly, currents were higher and peaks were better shaped; secondly, peak IIa was not present, therefore overlap with the second DNA peak was avoided, which was crucial for the interpretation of the interaction. At pH 4.6, in acetate buffer the SW voltammogram of the dsDNA multilayer biosensor had two oxidation peaks representing oxidation of deoxyguanosine (dG) and deoxyadenosine (dA) at potentials 1.05 V and 1.30 V, respectively (Fig. 6).

In a new experiment the SW voltammogram of 9Cl-A was recorded at bare GCE under the same conditions as when the dsDNA biosensor was used. For this purpose, bare GCE was immersed in a 1.0 × $10^{-4}$ M 9Cl-A solution for 5 min and then transferred to the electrochemical cell with acetate buffer at pH 4.6 where the voltammogram of adsorbed 9Cl-A at electrode surface was recorded. In Fig. 6 the SW voltammogram of adsorbed 9Cl-A (blue line) is presented together with the voltammogram obtained from the 1.0 × $10^{-4}$ M 9Cl-A solution (pH 4.6) (green line), showing the Ia oxidation peak with a lower current and slightly more positive potential, as expected when this transfer technique is applied. Both 9Cl-A voltammograms showed the absence of the IIa oxidation peak.

After the interaction of 9Cl-A in an incubated solution with DNA immobilized on the electrode surface, its morphology changed, which caused changes in dG and dA oxidation peaks. The interaction was initially detected after a 5 min incubation of the DNA biosensor in 1.0 × $10^{-4}$ M 9Cl-A solution [30]. Peaks Ia of 9Cl-A and dG of DNA overlapped and superimposed resulting in an increase in total current (Ia + dG, Fig. 7), making it difficult to distinguish between these two contributions. Therefore, only the change in dA peak was informative for clarifying the interaction. After incubation, peak dA was shifted to a more positive potential and its height decreased. In order to confirm that the decrease in the dA peak was due to the interaction with 9Cl-A, a control dsDNA-electrochemical biosensor was held in the buffer solution pH 4.6 for 30 min. As expected, no changes were detected in the DNA voltammogram.

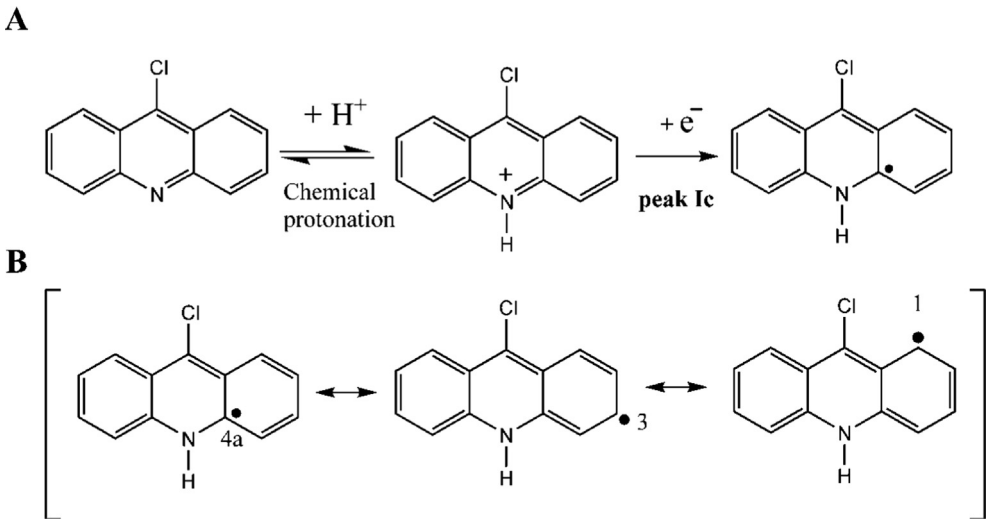


**Scheme 2.** (A) Proposed mechanism for reduction of 9Cl-A; (B) Resonance structures of 9Cl-A radical.

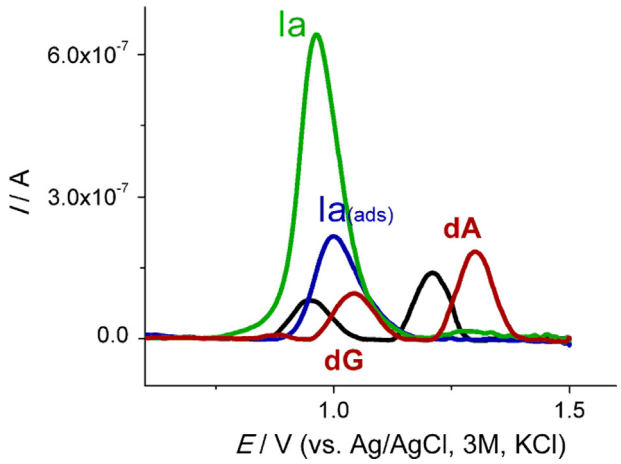


**Fig. 6.** SW baseline corrected voltammograms of: (——) dsDNA biosensor, pH 4.6; (——) dsDNA biosensor, pH 7.0; (——) 9Cl-A adsorbed from the solution, pH 4.6; (——) $1 \times 10^{-4}$ M 9Cl-A solution, pH 4.6.

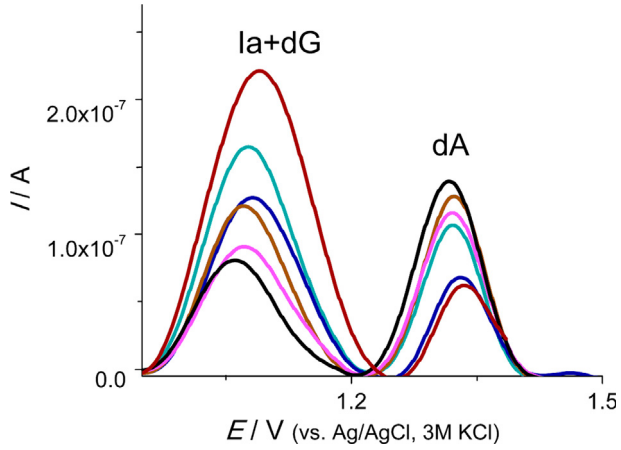


**Fig. 7.** SW baseline corrected voltammograms of 9Cl-A – DNA after interaction with different 9Cl-A concentration: (——) $1 \times 10^{-4}$ M, (——) $8 \times 10^{-6}$ M, (——) $5 \times 10^{-7}$ M, (——) $3.3 \times 10^{-7}$ M, (——) $1 \times 10^{-7}$ M, and (——) dsDNA biosensor; pH 4.6; ($t_{incubation}$ = 30 min).

The influence of interaction time (5, 10 and 30 min) between adsorbed DNA and $1.0 \times 10^{-4}$ M 9Cl-A in solution (pH 4.6) on dA and dG peak current was investigated in our previous work [30]. The optimum time for interaction was chosen (30 min) according to a very pronounced decrease in dA peak current ($\Delta I_p \approx 100$ nA). This was probably a result of 9Cl-A interaction with dA residues and the formation of DNA aggregates, as reported for other intercalating drugs [68]. Several chemotherapeutic agents [13,16,17,23] also interacted with DNA and caused a decrease in the dA peak which was, upon interaction, the consequence of impaired transfer of electrons to the electrode surface. A slight shift towards a more positive potential value suggested that the examined compounds intercalated into DNA.

The decrease in the dA peak (Fig. 7) indicated that during the interaction a ds-DNA structure could be distorted as a result of subtle damage by 9Cl-A. The changes in the current responses can be expressed as normalized peak current: d(dA)(%), using the equation:

$$d(dA)(\%) = 100 I_{p,dA}/I_{p0,dA} \quad (4)$$

where $I_{p,dA}$ and $I_{p0,dA}$ represent deoxyadenosine peak currents after and before interaction with 9Cl-A. The obtained results are summarized in Table 1. The normalized peak current decreased after a 30 min incubation time by > 50% when $1.0 \times 10^{-4}$ M 9Cl-A was used.

**Table 1**
The 9Cl-A–DNA interaction expressed by normalized values of the SW voltammetric responses and change in the dA peak potential for different incubation times ($c_{9Cl\text{-}A} = 1 \times 10^{-4}$ M).

| $t_{incubation}$ (min) | d(dA) (%) | $\Delta E_p$ (V) |
|---|---|---|
| 5 | 89.25 | 0.016 |
| 10 | 70.61 | 0.016 |
| 30 | 48.45 | 0.018 |

The phenomenon of the change in the nature of the interaction, from electrostatic to intercalative, with an increase of ionic strength was reported previously [69,70]. Based on those studies, the formal potential shift in the negative direction at low ionic strengths indicated that the behavior of the ds-DNA on the electrode surface was due to electrostatic interactions, while the formal potential shift in the positive direction at higher ionic strengths indicated intercalative interactions. According to our results [the shift of the dA peak potential of 0.018 V in the positive direction (Table 1)], the interaction between 9Cl-A and DNA could be characterized as intercalation.

According to previous results and discussions above, the interaction occurs between adsorbed DNA molecules on the surface of the electrode and the 9Cl-A from the incubation solution in which the incubation takes place. The aims of additional experiments were to investigate the concentration effect of the 9Cl-A incubation solutions on the interaction which resulted in formation of adsorbed supramolecular compound as well as to determine the lowest 9Cl-A concentration at which it was possible to detect interaction between DNA and 9Cl-A using SWV.

The decrease in dA peak current was used to examine the intensity of the interaction of dsDNA adsorbed onto the electrode surface and the different concentrations of incubation 9Cl-A solution ranging from $1.0 \times 10^{-7}$ M to $2.5 \times 10^{-4}$ M. The voltammograms presented at Fig. 7 showed that the anodic responses of the dA moiety changed with different concentration of 9Cl-A after a 30 min interaction. Fig. 8 shows two concentration ranges where the dA peak current showed linear dependence *v.* concentration. Sudden peak current decrease was evident at low concentrations indicating significant complex formation. As the 9Cl-A concentration increased, the peak current intensity stabilized. Accordingly, linear dependence with regression equations $Ip(A) = -0.038c(M) + 1.53 \times 10^{-7}$ ($R^2$ = 0.867) and $Ip(A) = -1.10 \times 10^{-4} c(M) + 8.44 \times 10^{-8}$ ($R^2$ = 0.920) were found for 9Cl-A concentration ranges $1.0 \times 10^{-7}$ M – $1.3 \times 10^{-6}$ M and $8.0 \times 10^{-6}$ M – $1.0 \times 10^{-4}$ M respectively (Fig. 8). At 9Cl-A concentrations higher than $1.0 \times 10^{-4}$ M dA peak current slightly increased ($2.5 \times 10^{-4}$ M, data not shown [31]) which might have been attributed to lower capability of 9Cl-A binding to electroactive DNA bases under these conditions.

The apparent binding constant of the supramolecular 9Cl-A-DNA complex, formed by the interaction between 9Cl-A in solution and dsDNA molecules adsorbed on the electrode surface, was determined. The concentration of dsDNA adsorbed on the electrode surface was constant whilst 9Cl-A concentration increased during the experiment. This modification of a standard titration procedure [71] was conducted assuming that only one type of complex was formed and that the process could be presented by the following equilibrium reaction:

$DNA_{ads} + n(9Cl\text{-}A) \leftrightarrow (9Cl\text{-}A)_n\text{–}DNA_{ads}$

and the corresponding equilibrium constant:

$$K = \frac{[(9Cl - A)_n - DNA_{ads}]}{[DNA_{ads}][9Cl - A]^n} \quad (5)$$

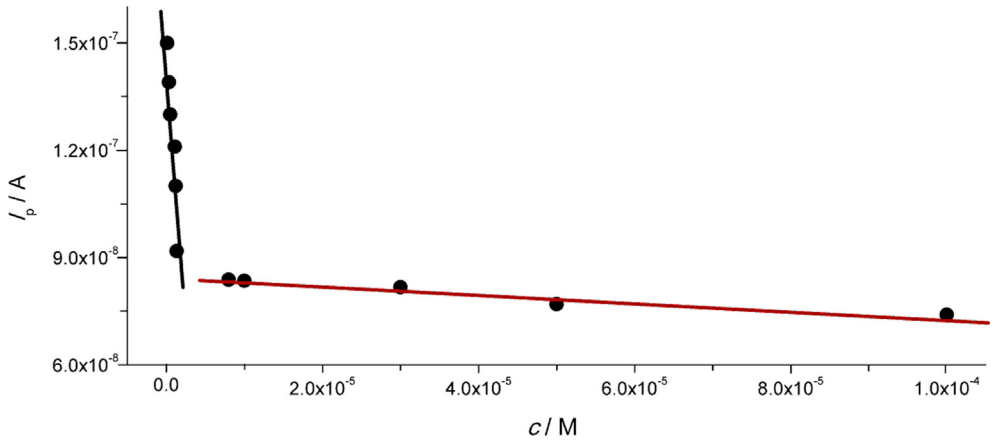


**Fig. 8.** Dependence of SWV dA peak current on the concentration of incubation 9Cl-A solutions (y = –0.038 × + 1.53 × $10^{-7}$; $R^2$ = 0.867 and y = –1.10 × $10^{-4}$ × + 8.44 × $10^{-8}$; $R^2$ = 0.920 for 9Cl-A concentration ranges 1.0 × $10^{-7}$ M – 1.3 × $10^{-6}$ M and 8.0 × $10^{-6}$ M – 1.0 × $10^{-4}$ M respectively).

Transforming the previous expressions, the following equation:

$$\log\left[\frac{I_{complex}}{I_{DNA}-I_{complex}}\right] = -n\log K - n\log c_{9Cl-A} \quad (6)$$

was obtained where $I_{DNA}$ and $I_{complex}$ represented dA peak currents in the absence of 9Cl-A and with different 9Cl-A concentrations forming the dsDNA-9Cl-A complex, respectively. Based on the obtained values for the slope ($n$ = 0.886 ≈ 1) and the intercept from the linear dependence $log\left[\frac{I_{complex}}{I_{DNA}-I_{complex}}\right]$ *vs.* $\log c_{9Cl-A}$ (Fig. 9) the value for the binding constant of the adsorbed complex was determined,

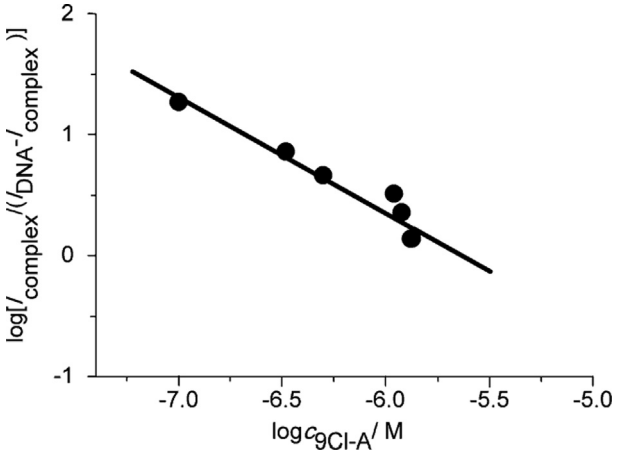


**Fig. 9.** Plot of $\log\left[\frac{I_{complex}}{I_{DNA}-I_{complex}}\right]$ *vs.* $\log c_{9Cl-A}$ dependence (y = – 0.886 × – 4.91; $R^2$ = 0.925).

$K$ = 3.45 × $10^5$ $M^{-1}$. The resulting binding constant was comparable with the values in the range $10^4$ – $10^6$ $M^{-1}$ reported for the other compounds and intercalating drugs [72–74] obtained using electrochemical and spectroscopic methods for complexes formed in solution. The $K$ value obtained in this work was greater in comparison to the binding constant for acridine orange intercalating into dsDNA ($K_{AO}$ = 2.69 × $10^4$ $M^{-1}$) determined using spectroscopic methods in neutral solution [72], which could be explained by easier interaction of the components when dsDNA is adsorbed.

By using the obtained binding constant of the complex between the adsorbed dsDNA and 9Cl-A, the change in the Gibbs free energy ($\Delta G$), representing a measure of the formed complex stability, was calculated according to the equation:

$$\Delta G = -RTlnK \quad (7)$$

(all the measurements were conducted at room temperature (25 °C). $\Delta G$ = – 31.55 kJ $mol^{-1}$ was obtained and the negative $\Delta G$ value confirmed the process spontaneity when the interaction occurred on the electrode surface between 9Cl-A and adsorbed dsDNA [56].

The lowest 9Cl-A concentration whose interaction with DNA was possible to detect using SWV was 1.0 × $10^{-7}$ M, confirming previously quoted references which stated SWV's advantages compared to other voltammetric methods.

### 3.5. Results of molecular docking analysis

According to previous investigations, the synthetic drug amsacrine (AMSA) has been proven to be an intercalating agent and acts as a topoisomerase II poison [44]. Amsacrine has an acridine core. Due to its mechanism of action and its structural similarity to 9Cl-A we used the DNA/amsacrine/topoisomerase II complex from PDB

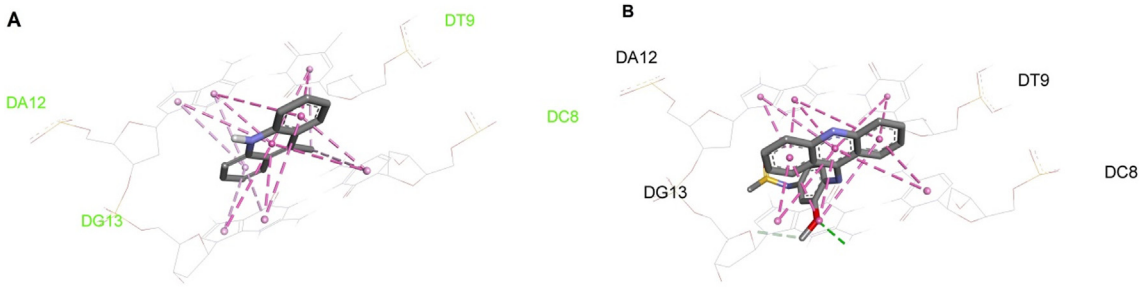


**Fig. 10.** Binding of 9Cl-A (A) and amsacrine (B) to dsDNA.

for our docking analysis. The docking analysis was performed to reveal binding interactions of 9Cl-A with DNA nucleotides. The binding energy of 9Cl-A (−7.7 kcal/mol) was similar to AMSA (−7.5 kcal/mol). The most significant interactions of 9Cl-A with DNA were between the acridine ring and DC8 (π – π stacked), DT9 (π – π stacked), DA12 (π – π stacked), DG13 (π – π stacked), DC8 (π –alkyl), DT9 (π – alkyl), DA12 (π – alkyl) and DG13 (π – alkyl). This study confirmed that intercalation between the base pairs was the most probable mode of 9Cl-A binding to DNA. The comparison of 9Cl-A and amsacrine binding interactions to dsDNA is shown in Fig. 10.

## 4. Conclusions

By applying cyclic, differential pulse and square wave voltammetry using a glassy carbon electrode, the electrochemical behavior of 9Cl-A was studied. A complex, pH-dependent, diffusion-controlled, irreversible redox process consisting of independent oxidation and reduction electrode reactions was revealed. Oxidation of 9Cl-A started with the formation of a cation radical monomer that rapidly underwent dimerization yielding a dimer that was oxidized by a second consecutive electron transfer forming new cation radical. The reduction of 9Cl-A produced radical monomers, that became stable after dimer formation. The glassy carbon electrode covered with three drops of dsDNA solution, representing electrochemical biosensor, was used to examine interaction between 9Cl-A and DNA. The interaction that occurred with surface immobilized dsDNA was characterised by the change in the dA oxidation peak position and by comparing the peak currents recorded before and after incubation.

These changes were followed by SW voltammetry. The most pronounced decrease in dA peak at pH 4.6 was observed with $1.0 \times 10^{-4}$ M 9Cl-A after a 30 min incubation. The lowest 9Cl-A concentration whose interaction with DNA was possible to detect using SWV was $1.0 \times 10^{-7}$ M. Different concentrations of 9Cl-A ($1.0 \times 10^{-7}$ M – $1.0 \times 10^{-4}$ M) were used to calculate the binding constant ($K$ = 3.45 × $10^5$ $M^{-1}$). The negative value of Gibbs free energy change suggested that the formation of the adsorbed 9Cl-A–DNA complex occurred spontaneously. A very stark decrease in dA peak intensity, together with slight shift of potential towards a more positive value, suggested that the interaction occurred via intercalation of 9Cl-A within double strands of DNA. Experimental data were supported by the molecular docking analysis. It may be assumed that 9Cl-A intercalates into DNA strands and leads to more rigid structure formation, causing condensation of dsDNA.

The novelty of our work is that it provides insight into the redox mechanism, dimer formation and detailed electrochemical properties, during the 9Cl-A - DNA interaction and nature of the complex formed, using simple electroanalytical methodology. The ability to form a complex with DNA promotes 9Cl-A as a candidate to be a precursor for drug design, synthesis and pharmaceutical development of new antitumor agents.

## Declaration of Competing Interest

The authors declare that they have no known competing financial interests or personal relationships that could have appeared to influence the work reported in this paper.

## Acknowledgements

This work was supported by the Ministry of Education, Science and Technological Development of the Republic of Serbia, Projects No. 172033 and 172041. The authors are grateful to prof. dr Vladimir Savić for his assistance in redox mechanism elucidation and clarification. Special thanks to Dr. David R. Jones for his diligent proofreading of this paper.

## Appendix A. Supplementary data

Supplementary data to this article can be found online at https://doi.org/10.1016/j.bioelechem.2020.107579.

## References

[1] P. Belmont, J. Bosson, T. Godet, M. Tiano, Acridine and acridone derivates, anticancer properties and synthetic methods: where are we now? Anti–cancer Agents Med, Chem. 7 (2007) 139–169, https://doi.org/10.2174/187152007780058669.
[2] J.S. Rupar, V.D. Dobričić, M.M. Aleksić, J.S. Brborić, O.A. Čudina, A review of published data on acridine derivatives with different biological activities, Kragujevac J. Sci. 40 (2018) 83–101, https://doi.org/10.5937/KgJSci1840083R.
[3] R.J. Harrison, J. Cuesta, G. Chessari, M.A. Read, S.K. Basra, A.P. Reszka, J. Morrell, S.M. Gowan, C.M. Incles, F.A. Tanious, W.D. Wilson, L.R. Kelland, S. Neidle, Trisubstituted acridine derivatives as potent and selective telomerase inhibitors, J. Med. Chem. 46 (2003) 4463–4476, https://doi.org/10.1021/jm0308693.
[4] R.A. Hutchins, J.M. Crenshan, D.E. Graves, W.A. Denny, Influence of substituent modification on DNA binding energetics of acridine-based anticancer agents, Biochemistry 42 (2003) 13754–13761, https://doi.org/10.1021/bi035434w.
[5] S.A. Lyakhov, Y.I. Suveyzdis, O.V. Bykhovskaya, N.M. Isko, S.A. Andronati, L.A. Litvinova, Biological active acridine derivatives. 3. Acridinylaminoacids and their esters: synthesis and cytostatic activity, Pharmazie 52 (1997) 560–561.
[6] A. Erdem, M. Ozsoz, Electrochemical DNA Biosensors Based on DNA-Drug Interactions, Electroanal. 14 (2002) 965–974, https://doi.org/10.1002/1521-4109(200208)14:14<965::AID-ELAN965>3.0.CO;2-U.
[7] J. Labuda, A.M. Oliveira-Brett, G. Evtugyn, M. Fojta, M. Mascini, M. Ozsoz, I. Palchetti, E. Paleček, J. Wang, Electrochemical nucleic acid-based biosensors: concepts, terms, and methodology (IUPAC Technical Report), Pure Appl. Chem. 82 (2010) 1161–1187, https://doi.org/10.1351/PAC-REP-09-08-16.
[8] J. Labuda, V. Vyskocil, DNA/Electrode Interface, Detection of damage to DNA using DNA modified electrodes, in: G. Kreysa, K. Ota, R. F. Savinell (Eds.), Encyclopedia of Applied Electrochemistry, Springer, New York, 2014 p. 346–352. https://doi.org/10.1007/978-1-4419-6996-5_259
[9] V.C. Diculescu, A.M.C. Paquim, A.M.O. Brett, Electrochemical DNA sensors for detection of DNA damage, Sensors 5 (2005) 377–393, https://doi.org/10.3390/s5060377.
[10] M.M. Aleksić, V. Kapetanović, An overview of the optical and electrochemical methods for detection of DNA - drug interactions, Acta Chim. Slov. 61 (2014) 555–573.
[11] A.-M. Chiorcea-Paquim, O. Corduneanu, S.C.B. Oliveira, V.C. Diculescu, A.M. Oliveira-Brett, Electrochemical and AFM evaluation of hazard compounds–DNA interaction, Electrochim. Acta 54 (2009) 1978–1985, https://doi.org/10.1016/j.electacta.2008.07.032.
[12] S.C.B. Oliveira, A.M. Chiorcea-Paquim, S.M. Ribeiro, A.T.P. Melo, M. Vivan, A.M. Oliveira-Brett, In situ electrochemical and AFM study of thalidomide–DNA interaction, Bioelectrochemistry 76 (2009) 201–207, https://doi.org/10.1016/j.bioelechem.2009.03.003.
[13] S. Kurbanoglu, B. Dogan-Topal, L. Hlavata, J. Labuda, S.A. Ozkan, B. Uslu, Electrochemical investigation of an interaction of the antidepressant drug aripiprazole with original and damaged calf thymus dsDNA, Electrochim. Acta 169 (2015) 233–240, https://doi.org/10.1016/j.electacta.2015.04.087.
[14] B. Dogan-Topal, S.A. Ozkan, A novel sensitive electrochemical DNA biosensor for assaying of anticancer drug leuprolide and its adsorptive stripping voltammetric determination, Talanta 83 (2011) 780–788, https://doi.org/10.1016/j.talanta.2010.10.049.
[15] I.C. Lopes, S.C.B. Oliveira, A.M. Oliveira-Brett, In situ electrochemical evaluation of anticancer drug temozolomide and its metabolites-DNA interaction, Anal. Bioanal. Chem. 405 (2013) 3783–3790, https://doi.org/10.1007/s00216-012-6546-x.
[16] A. Erdem, B. Kosmider, R. Osiecka, E. Zyner, J. Ochocki, M. Ozsoz, Electrochemical genosensing of the interaction between the potential chemotherapeutic agent, cis-bis(3-aminoflavone)dichloroplatinum(II) and DNA in comparison with cis-DDP, J. Pharmaceut. Biomed. 38 (2015) 645–652, https://doi.org/10.1016/j.jpba.2005.02.010.
[17] D. Ozkan, H. Karadeniz, A. Erdem, M. Mascini, M. Ozsoz, Electrochemical genosensor for Mitomycin C-DNA interaction based on guanine signal, J. Pharmaceut. Biomed. 35 (2004) 905–912, https://doi.org/10.1016/j.jpba.2004.03.001.
[18] B. Dogan-Topal, B. Uslu, S.A. Ozkan, Voltammetric studies on the HIV-1 inhibitory drug efavirenz: The interaction between dsDNA and drug using electrochemical DNA biosensor and adsorptive stripping voltammetric determination on disposable pencil graphite electrode, Biosens. Bioelectron. 24 (2009) 2358–2364, https://doi.org/10.1016/j.bios.2008.12.005.
[19] V.C. Diculescu, A.M. Oliveira-Brett, In situ electrochemical evaluation of dsDNA interaction with the anticancer drug danusertib nitrenium radical product using the DNA-electrochemical biosensor, Bioelectrochemistry 107 (2016) 50–57, https://doi.org/10.1016/j.bioelechem.2015.10.004.

[20] Burcu Dogan-Topal, Burcin Bozal-Palabiyik, Sibel A. Ozkan, Bengi Uslu, Investigation of anticancer drug lapatinib and its interaction with dsDNA by electrochemical and spectroscopic techniques, Sensors and Actuators B: Chemical 194 (2014) 185–194, https://doi.org/10.1016/j.snb.2013.12.088.
[21] K. Nemčeková, J. Labuda, V. Milata, J. Blaškovičová, J. Sochr, Interaction of DNA and mononucleotides with theophylline investigated using electrochemical biosensors and biosensing, Bioelectrochemistry 123 (2018) 182–189, https://doi.org/10.1016/j.bioelechem.2018.05.004.
[22] V. Svitková, M. Hanzelyová, H. Macková, J. Blaškovičova, V. Vyskočil, Dana Farkašová. J. Labuda, Behaviour and detection of acridine-type DNA-based biosensor with the protective polyvinyl alcohol membrane, J. Electroanal. Chem. 821 (2018) 87−91. https://doi.org/10.1016/j.jelechem.2017.11.028
[23] A.D.R. Pontinha, S. Sparapani, S. Neidle, A.M. Oliveira-Brett, Triazole–acridine conjugates: Redox mechanisms and in situ electrochemical evaluation of interaction with double-stranded DNA, Bioelectrochemistry 89 (2013) 50–56, https://doi.org/10.1016/j.bioelechem.2012.08.005.
[24] M. Fojta, A. Daňhel, L. Havran, V. Vyskočil, Recent progress in electrochemical sensors and assays for DNA damage and repair, TrAC–Trend, Anal. Chem. 79 (2016) 160–167, https://doi.org/10.1016/j.trac.2015.11.018.
[25] M.M. Aleksić, V. Kapetanović, Electrochemical biosensors as a tool for the investigation of DNA structure, damage and interaction with other molecules, Facta Universitatis, Series: Physics, Chemistry and Technology 11 (2013) 27–43, https://doi.org/10.2298/FUPCT1301027A.
[26] A.M. Oliveira-Brett, Electrochemistry for probing DNA damage, in: C.A. Grimes, E.C. Dickey, M.V. Pishko (Eds.), Encyclopedia of Sensors, American Scientific Publishers, USA, 2006, pp. 301–314.
[27] A. Hájková, J. Barek, V. Vyskočil, Voltammetric Determination of 2-aminofluoren-9-one and investigation of its interaction with DNA on a glassy carbon electrode, Electroanal. 27 (2015) 101–110.
[28] V.C. Diculescu, R.M. Barbosa, A.M. Oliveira-Brett, In situ sensing of DNA damage by a nitric oxide-releasing compound, Anal. Lett. 38 (2005) 2525–2540, https://doi.org/10.1080/00032710500369737.
[29] S.C.B. Oliveira, A.M. Oliveira-Brett, DNA-electrochemical biosensors: AFM surface characterisation and application to detection of in situ oxidative damage to DNA, Comb. Chem. High. T. Scr. 13 (2010) 628–640, https://doi.org/10.2174/138620731100407062 8.
[30] J. Pantić, M. M. Aleksić, V. Dobričić, O. Čudina, J. Brborić, S. Vladimirov, Electrochemical oxidation and interaction of 9-chloroacridine with DNA at glassy carbon electrode, in: 13th International Conference on Fundamental and Applied Aspects of Physical Chemistry 2016, Belgrade, Serbia 26-30 September 2016, Vol. 1, Society of Physical Chemists of Serbia, 383−386
[31] J. Rupar, M. Aleksić, V. Dobričić, O. Čudina, J. Brborić, S. Vladimirov, Application of electrochemical biosensor for investigation of acridine derivatives – DNA interaction, in: 14th International Conference on Fundamental and Applied Aspects of Physical Chemistry 2018, Belgrade, Serbia 24-28 September 2018, Vol. 1, Society of Physical Chemists of Serbia, 379−382.
[32] J. Barek, J. Matějka, J. Zima, Determination of acridine, benz[c]acridine and dibenz[a, h]acridine by fast scan differential pulse voltammetry and adsorptive stripping voltammetry, Collect. Cyech. Chem. C. 59 (1994) 294–308, https://doi.org/10.1135/cccc19940294.
[33] S.T. Girousi, D.K. Alexiadou, A.K. Ioannou, An electroanalytical study of the drug proflavine, Microchim. Acta 160 (2008) 435–439, https://doi.org/10.1007/s00604-007-0812-1.
[34] I.Ch. Gherghi, S.T. Girousi, A.N. Voulgaropoulos, R. Tzimou-Tsitouridou, DNA modified carbon paste electrode applied to the voltammetric study of the interaction between DNA and acridine orange, Chem. Anal-Warsaw 49 (2004) 467–480.
[35] R.N. Adams, Electrochemistry at solid electrodes, Marcel Dekker Inc., New York, 1969, pp. 319–322.
[36] K. Yasukouchi, I. Taniguchi, H. Yamaguchi, K. Arakawa, Anodic oxidation of acridine in acetonitrile, J. Electroanal. Chem. 121 (1981) 231–240, https://doi.org/10.1016/S0022-0728(81)80581-5.
[37] Š. Komorsky-Lovrić, V. Mirčeski, F. Scholz, Voltammetry of organic microparticles, Microchim. Acta 132 (1999) 67–77, https://doi.org/10.1007/PL00010075.
[38] V.D. Bezuglyi, M.B. Sidom, V.A. Shapovalov, A.N. Gaidukevich, Polarographic study of acridine and 9-chloroacridine and its derivatives in dimethylformamide, Chem. Heterocycl. Compd. 14 (1978) 1350–1354, https://doi.org/10.1007/BF00487405.
[39] R.C. Kaye, H.I. Stonehill, A polarographic study of the electroreduction of acridine, J. Chem. Soc. (1951) 27–38, https://doi.org/10.1039/JR9510000027.
[40] D.D. Perrin, B. Dempsey, Buffers of pH and metal ion control, Laboratory Manuals, Chapman and Hall, London, 1974.
[41] A.D.R. Pontinha, S.M.A. Jorge, V.C. Diculescu, M. Vivan, A.M. Oliveira-Brett, Antineoplastic drug methotrexate redox mechanism using a glassy carbon electrode, Electroanal. 24 (2012) 917–923.
[42] A. M. Oliveira-Brett, V. C. Diculescu, A. M. Chiorcea-Paquim and S. H. P. Serrano, DNA-electrochemical biosensors for investigating DNA damage, Chapter 20 in: S. Alegret and A. Merkoci (Eds) Electrochemical sensor Analysis, Elsevier B. V. Amsterdam The Nederlands, Comprehensive Analytical Chemistry, 49 (2007) 413−438. https://doi.org/10.1016/S0166-526X(06)49020-6.
[43] V. Vyskočil, M. Blašková, A. Hájková, E. Horáková, Z. Krejčová, K. Stávková1, and J. Wang, Electrochemical DNA biosensors – Useful diagnostic tools for the detection of damage to DNA caused by organic xenobiotics (A Review), Chapter 9 in: K. Kalcher, R. Metelka, I. Švancara, K. Vytřas (Eds.), Sensing in Electroanalysis, University Press Centre, Pardubice, Czech Republic, 7 (2012) 141−162.
[44] C.G. Jensen, W.R. Wilson, A.R. Bleumink, Effects of amsacrine and other DNA-intercalating drugs on nuclear and nucleolar structure in cultured V79 Chinese hamster cells and PtK2 rat kangaroo cells, Cancer Res. 2 (1985) 717–725. http://cancerres.aacrjournals.org/content/45/2/717.
[45] C.C. Wu, Y.C. Li, Y.R. Wang, T.K. Li, N.L. Chan, On the structural basis and design guidelines for type II topoisomerase-targeting anticancer drugs, Nucleic Acids Res. 41 (2013) 10630–10640, https://doi.org/10.1093/nar/gkt828.
[46] Discovery Studio Visualizer 4.5.0, 2005-2015, Dassault Systèmes, Vélizy-Villacoublay, France.
[47] O. Trott, A.J. Olson, Software News and Update AutoDockVina: Improving the speed and accuracy of docking with a new scoring function, efficient optimization, and multithreading, J. Comput. Chem. 31 (2010) 455–461, https://doi.org/10.1002/jcc.21334.
[48] M.M. Aleksić, V. Radulović, D. Agbaba, V. Kapetanović, An extensive study of electrochemical behavior of brimonidine and its determination at glassy carbon electrode, Electrochim. Acta 106 (2013) 75–81.
[49] C. M. A. Brett, A. M. Oliveira-Brett, Electrochemistry principles, Methods and Applications, Oxford University Press, UK, 1993. https://doi.org/10.1002/bbpc.19940981033.
[50] R. G. Compton, C. E. Banks, In: Understanding Voltammetry, 2nd edition, Imperial College Press, 2010. https://doi.org/10.1142/p726.
[51] E. Nosheen, A. Shah, A. Badshah, Z. Rehman, H. Hussian, R. Qureshi, S. Ali, M. Siddig, A.M. Khan, Electrochemical oxidation of hydantoins at glassy carbon electrode, Electrochim. Acta 80 (2012) 108–117, https://doi.org/10.1016/j.electacta.2012.06.116.
[52] P.A. Mabrouk, Direct Electrochemistry for the imidazole complex of microperoxidase-11 in dimethyl sulfoxide solution at naked electrode substrates including glassy carbon, gold and platinum, Anal. Chem. 68 (1996) 189–191, https://doi.org/10.1021/ac950792t.
[53] A.H. Shah, A. Shah, U.A. Rana, S.U.-D. Khan, H. Hussain, S.B. Khan, R. Qureshi, A. Badshah, Redox mechanism and evaluation of kinetic and thermodynamic parameters of 1,3-dioxolo[4,5-g]pyrido[2,3-b]- quinoxaline using electrochemical techniques, Electroanal. 26 (2014) 2292–2300, https://doi.org/10.1002/elan.201400324.
[54] A.J. Bard, L.R. Faulkner, Electrochemical methods: Fundamentals and Applications, John Wiley & Sons, Chichester, 2001.
[55] S. Sampath, O. Lev, Electrochemical oxidation od NADH on sol-gel derived, surface renewable, non-modified and mediator modified composite-carbon electrodes, J. Electroanal. Chem. 446 (1998) 57–65, https://doi.org/10.1016/S0022-0728(97)00547-0.
[56] J. Rupar, M.M. Aleksić, K. Nikolić, M.R. Popović-Nikolić, Comparative electrochemical studies of kinetic and thermodynamic parameters of Quinoxaline and Brimonidine redox process, Electrochim. Acta 271 (2018) 220–231, https://doi.org/10.1016/j.electacta.2018.03.114.
[57] C.P. Andrieux, J.M. Saveant, Dimerization, disproportionation and e.c.e. mechanisms in the reduction of imines in acetonitrile and dimethyl-formamide, J. Electroanal. Chem. 33 (1971) 453–461, https://doi.org/10.1016/S0022-0728(71)80128-6.
[58] J. Wang, Analytical Electrochemistry, 3rd edition., Wiley-VCH, Hoboken, New Jersey, 2006.
[59] M.A. Arugula, Y. Zhang, A.L. Simonian, Biosensors as 21st century technology for detecting genetically modified organisms in food and feed, Anal. Chem. 86 (2014) 119–129, https://doi.org/10.1021/ac402898j.
[60] Y. Wang, E. Laborda, R.G. Compton, Electrochemical oxidation of nitrite: Kinetic, mechanistic and analytical study by square wave voltammetry, J. Electroanal. Chem. 670 (2012) 56–61, https://doi.org/10.1016/j.jelechem.2012.02.016.
[61] C. Wu, A. Shah, H. Ye, X. Chen, J. Ye, H. Jiang, B. Chen, X. Wang, H. Yan, Droplet electrochemical study of the pH dependent redox behavior of novel ferrocenyl-carborane derivatives and its application in specific cancer cell recognition, Anal. Chim. Acta 857 (2015) 39–45, https://doi.org/10.1016/j.aca.2014.12.019.
[62] U. Amjad, A. Lashin, R. Abbasi, U. Ali Rana, N. Al-Arifi, G.S. Khan, S. Ali, H.-B. Kraatz, A. Shah, pH and temperature responsive electrooxidation of thiazole derivatives and preliminary screening of their antioxidant activity, J. Electrochem. Soc. 163 (2016) H350–H358, https://doi.org/10.1149/2.0021606jes.
[63] A.D.R. Pontinha, S.C.B. Oliveira, A.M. Oliveira-Brett, Electrochemical oxidation of metolazone at a glassy carbon electrode, Electroanal. 20 (2008) 2531–2536, https://doi.org/10.1002/elan.200804352.
[64] D. Kul, B. Dogan-Topal, S.A. Ozkan, B. Uslu, Poly(acridine orange)-modified glassy carbon electrodes: electrosynthesis, characterisation and sensor application with uric acid, J. Appl. Electrochem. 44 (2014) 831–840, https://doi.org/10.1007/s10800-014-0691-1.
[65] B. Dogan-Topal, S.A. Ozkan, B. Uslu, The analytical applications of square wave voltammetry on pharmaceutical analysis, Open Chem. Biomed. Methods J. 3 (2010) 56–73, https://doi.org/10.2174/1875038901003010056.
[66] C. M. A. Brett, A. M. Oliveira-Brett, Electrochemistry: Principles, Methods, and Applications, 1st edition, Oxford Science University Publications, Oxford, UK, 1993.
[67] A.M. Oliveira-Brett, J.A.P. Piedade, L.A. Silva, V.C. Diculescu, Electrochemical determination of all DNA nucleotides, Anal. Biochem. 332 (2004) 321–329, https://doi.org/10.1016/j.ab.2004.06.021.
[68] P.V.F. Santos, I.C. Lopes, V.C. Diculescu, A.M. Oliveira-Brett, DNA – cyanobacterial hepatotoxins microcystin-lr and nodularin interaction: electrochemical evaluation, Electroanal. 24 (2012) 547–553, https://doi.org/10.1002/elan.201100516.

[69] V. Radulović, M.M. Aleksić, V. Kapetanović, An electrochemical study of the adsorptive behaviour of Varenicline and its interaction with DNA, J. Serb. Chem. Soc. 77 (2012) 1409–1422, https://doi.org/10.2298/JSC120420073R.
[70] D.W. Pang, H.D. Abruna, Micromethod for the investigation of the interactions between DNA and redox-active molecules, Anal. Chem. 70 (1998) 3162–3169, https://doi.org/10.1021/ac980211a.
[71] Q. Feng, N.-Q. Li, Y.-Y. Jiang, Electrochemical studies of porphyrin interacting with DNA and determination of DNA, Anal. Chim. Acta 344 (1997) 97–104, https://doi.org/10.1016/S0003-2670(97)00008-1.
[72] S. Nafisi, A.A. Saboury, N. Keramat, J.F. Neault, H.A. Tajmir-Riahi, Stability and structural features of DNA intercalation with ethidium bromide, acridine orange and methylene blue, J. Mol. Struct. 827 (2007) 35–43, https://doi.org/10.1016/j.molstruc.2006.05.004.
[73] T.M. Ibrahim, H. Ibrahim, Interactions of an anticancer drug lomustine with single and double stranded DNA at physiological conditions analyzed by electrochemical and spectroscopic methods, J. Electroanal. Chem. 769 (2016) 62–71, https://doi.org/10.1016/j.jelechem.2016.03.020.
[74] K. Morawska, T. Popławski, W. Ciesielski, S. Smarzewska, Electrochemical and spectroscopic studies of the interaction of antiviral drug Tenofovir with single and double stranded DNA, Bioelectrochemistry 123 (2018) 227–232, https://doi.org/10.1016/j.bioelechem.2018.06.002.